Electronic Supplementary Information

Experimental section

Materials: Manganese nitrate ($Mn(NO_3)_2$) solution (50%), cobaltous nitrate ($Co(NO_3)_2·6H_2O$, 98.5%) and hydrazine hydrate ($N_2H_4·H_2O$, 90%) were purchased from Kelong chemical Ltd. in Chengdu. Ammonium (NH_4F, 96%), urea (99%), and sodium tellurite (Na_2TeO_3, 99%) were purchased from Aladdin Ltd. (Shanghai, China). $RuCl_3·3H_2O$ (43%) were bought from Sigma-Aldrich Chemical Reagent Co., Ltd. Ti mesh (TM) was provided by Hangxu Filters Flag Store, Hengshui, Hebei. The water used throughout all experiments was purified through a Millipore system. All the chemicals in the experiments were analytical grade and used without further treatments.

Preparation of Co–Mn–OH/TM and $CoTe_2$–$MnTe_2$/TM: Ti mesh possesses negligible HER activity, acceptable electronic conductivity, open structure allowing solvent good access at the reaction interface and ability to facilitate adhesion of the materials, which is a suitable substrate for growing active catalysts. The Co–Mn bimetallic hydroxide nanowire array on TM was prepared as follows, 2 mmol of $Mn(NO_3)_2·4H_2O$ (0.72 g), 4 mmol $Co(NO_3)_2·6H_2O$ (1.16 g), 24 mmol urea (1.45 g) and 10 mmol NH_4F (0.37 g) were dissolved in 70 mL distilled water. After stirring for 10 min, the clear solution was transferred to a 100 mL Teflon-lined stainless steel autoclave and a piece of pre-treated Ti mesh (2 × 4 cm) was immersed into the solution. The autoclave was sealed and maintained at 120 °C for 5 h in an electric oven. After cooled down to room temperature, the resulting Co–Mn precursor was washed with water under sonication, followed by drying at 60 °C. For the synthesis of $CoTe_2$–$MnTe_2$ hybrid nanowire array on TM**,** 2 mM of Na_2TeO_3 was dissolved by 70 mL of water. Then 10 mL of $N_2H_4·H_2O$ was added into the solution under vigorous stirring. The solution was transferred to a 100 mL Teflon-lined stainless steel autoclave and the as-obtained Co–Mn–OH/TM was immersed into the solution. The autoclave was sealed and maintained at 180 °C for 24 h in an electric oven. After cooled down to room temperature, the product was washed with water under sonication, followed by drying at 60 °C. For comparison, we prepared four other samples with different mole ratios of Co and Mn (1:1, 1:2, 1:0 and 0:1) under the same conditions, which are denoted as $CoTe_2$–$MnTe_2$/TM–1, $CoTe_2$–$MnTe_2$/TM–2, $CoTe_2$/TM, and $MnTe_2$/TM.

Synthesis of RuO_2 electrode: In a typical synthesis, 2.61 g of $RuCl_3·3H_2O$ and 30 mL of KOH were added into 100 mL of distilled water and stirred for 45 min at 100 °C. Then the solution was centrifuged and washed to obtain the precipitates. Finally, the precursor was dried at 80 °C overnight and then annealed at 300 °C in air atmosphere for 3 h. To synthesize RuO_2 supported on

TM, 20 mg of obtained RuO_2 was dispersed in 1 mL ethane/water (v:v = 1:1) solution under sonication for 30 min. Then 24.5 μL of catalytic inks were dropped on Ti mesh (0.5 × 0.5 cm), and dried at 80 °C for 4 h.

Characterizations: X-ray diffraction (XRD) patterns were performed using a LabX XRD-6100 X-ray diffractometer (SHIMADZU, Japan) with Cu Kα radiation ($\lambda = 1.5418$ Å) at 40 kV and 40 mA. Scanning electron microscopy (SEM) images were collected on a XL30 ESEM FEG scanning electron microscope at an accelerating voltage of 20 kV. The elemental mapping was carried out on a field-emission scanning electron microscope (FESEM, Hitachi S4800) equipped with an energy dispersive X-ray spectrometer (EDX). Transmission electron microscopy (TEM) images were made on a HITACHI H-8100 electron microscopy with an accelerating voltage of 200 kV. X-ray photoelectron spectroscopy (XPS) measurements were performed on an ESCALABMK II X-ray photoelectron spectrometer using Mg as the exciting source. Elemental analysis was performed to determine actual weight loading of Co and Pt by the inductively coupled plasma atomic emission spectroscopy (ICP-AES).

Electrochemical measurements: Electrochemical measurements were performed by a CHI 660E electrochemical analyzer (CH Instruments, Inc.) with a standard three-electrode system using $CoTe_2$–$MnTe_2$/TM as the working electrode, graphite plate as the counter electrode and Hg/HgO as the reference electrode. Prior to each electrochemical test, the KOH solutions were purged with nitrogen for 30 min. Linear sweep voltammetry curves were obtained at a scan rate of 5 mV s^{-1}. The long-term durability test was performed using chronoamperometric measurement. All potentials measured were calibrated to RHE using the following equation: E (RHE) = E (Hg/HgO) + 0.059 pH + 0.098 V. The potential was based on iR correction using the equation: $E(iR\text{-corrected}) = E - iR$, where i is the current and R is the uncompensated electrolyte ohmic resistance measured by electrochemical impedance spectroscopy. Electrochemical impedance spectroscopy measurements were carried out in the frequency range of 10^5 to 0.01 Hz and the magnitude of the modulation signal was 5 mV. The geometric surface area is calculated to 0.5 × 0.5 cm^2. All experiments were carried out at 25 °C.

Faradaic efficiency measurements:

The FE was calculated by comparing the amount of measured oxygen generated by potentiostatic anodic electrolysis with calculated O_2 (assuming 100% FE). The theoretical O_2 is calculated from the total charge during the electrolysis:

$$n_{O2} = Q/4F \qquad (1)$$

where n_{O2} (mol) is the mole of theoretical O_2, F (96485 C mol^{-1}) is the Faraday constant, 4 is denoted as two electrons needed to produce one O_2 molecule, and Q (C) is the electric quantity during the electrolysis. The generated oxygen was determined by gas chromatography equipped with a thermal conductivity detector at the potential of 1.55 V. Pressure data during electrolysis were recorded using a CEM DT-8890 differential air pressure gauge manometer data logger meter tester with a sampling interval of 1 point per second.

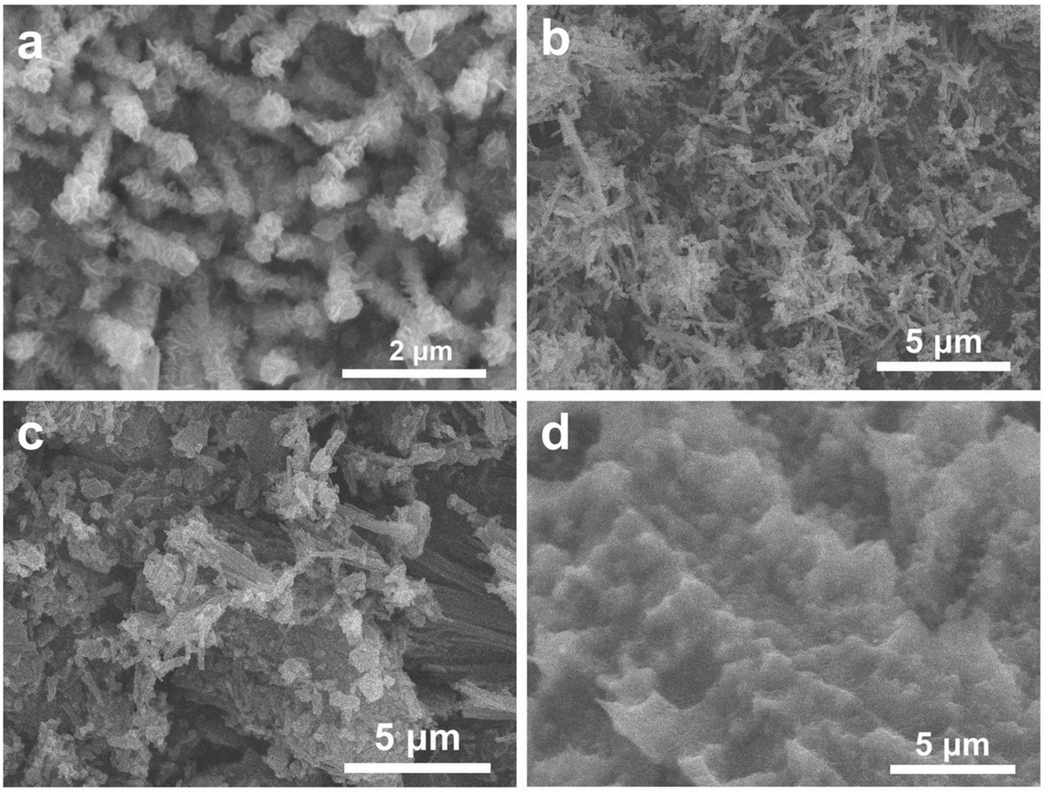

Fig. S1 SEM images of as-prepared samples. (a) $CoTe_2$/TM, (b) $CoTe_2$–$MnTe_2$/TM–1, (c) $CoTe_2$–$MnTe_2$/TM–2), and (d) $MnTe_2$/TM.

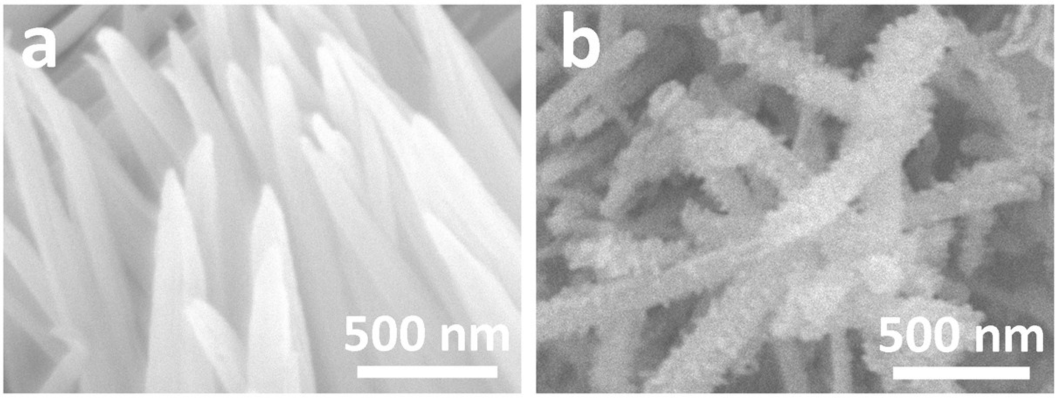

Fig. S2 SEM images of Co–Mn–OH/CC (a) and $CoTe_2$–$MnTe_2$/CC (b).

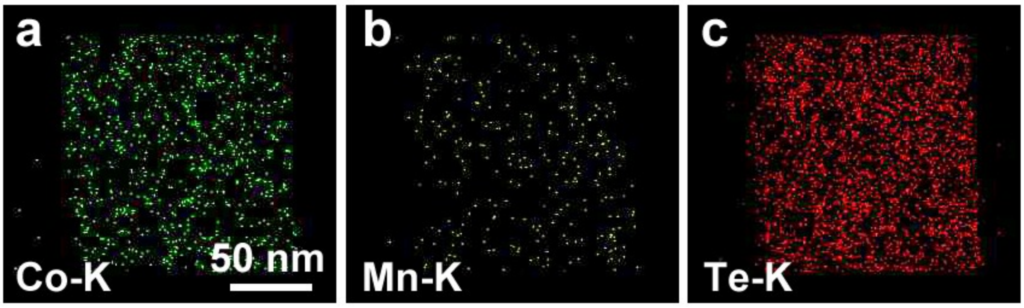

Fig. S3 EDX elemental mapping of $CoTe_2$–$MnTe_2$/TM.

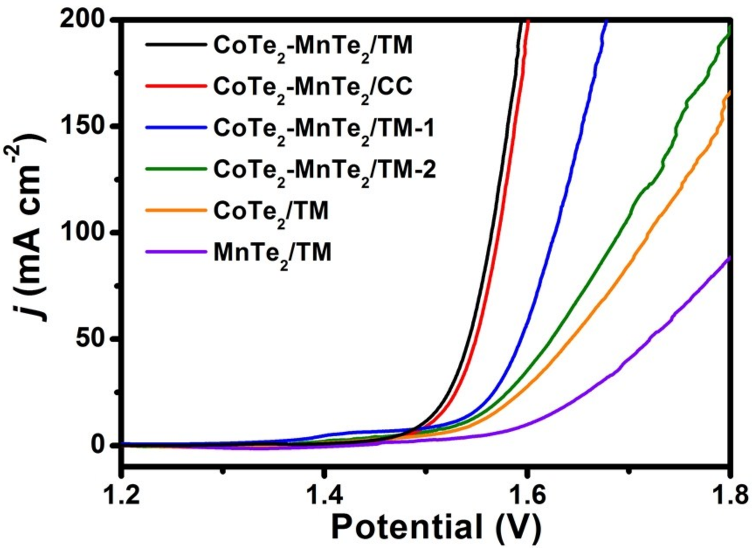

Fig. S4 LSV curves of as-prepared samples at a scan rate of 5 mV s^{-1}.

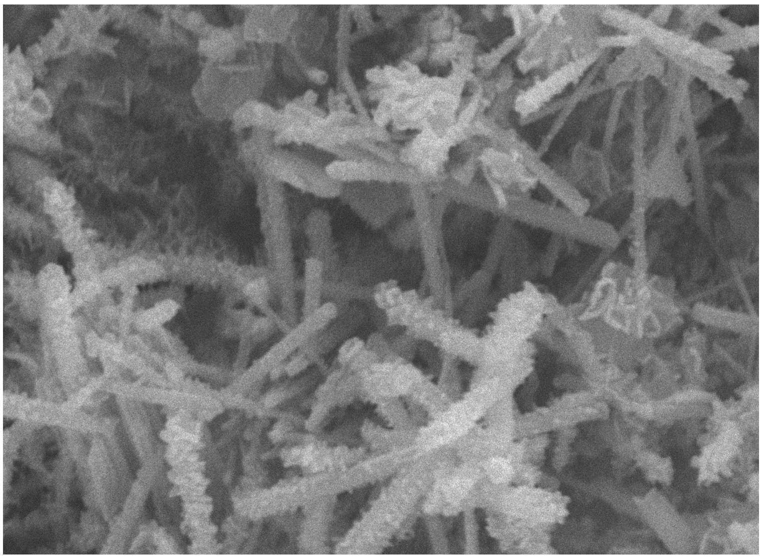

Fig. S5 SEM image of $CoTe_2$–$MnTe_2$/TM after stability test.

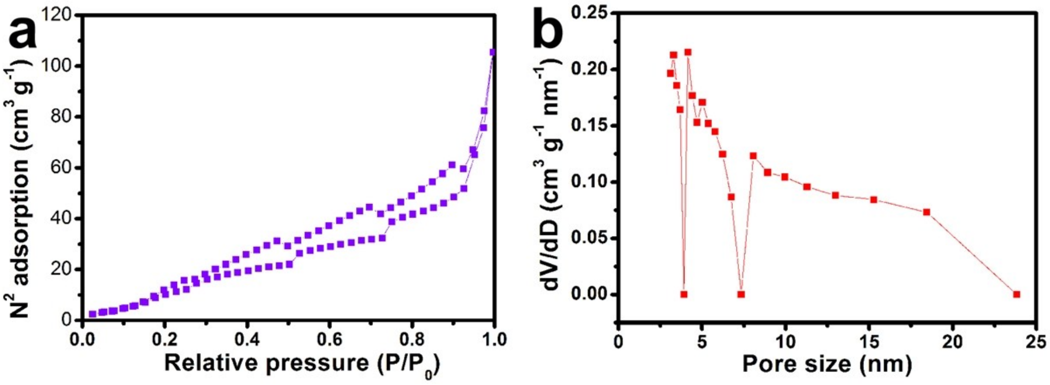

Fig. S6 (a) Nitrogen sorption and (b) corresponding pore size distribution of $CoTe_2$–$MnTe_2$.

Table S1. Comparison of OER performance for $CoTe_2$–$MnTe_2$/TM with other recently reported catalysts.

Catalyst	Electrolyte	j (mA cm^{-2})	η (mV)	Ref.
$CoTe_2$–$MnTe_2$/TM	**1.0 M KOH**	**50**	**310**	**This work**
$CoTe_2$@N-GC	1.0 M KOH	50	~375	1
$CoTe_2$/CNT–0.50	1.0 M KOH	50	~315	2
$CoTe_2$	1.0 M KOH	50	~465	3
$MnCo_2S_4$ NA/TM	1.0 M KOH	50	325	4
Co_3O_4 nanocrystal/carbon paper	1.0 M KOH	50	420	5
Co-S nanosheets	1.0 M KOH	50	410	6
NiCo LDH	1.0 M KOH	50	440	7
Hierarchical $Zn_xCo_{3-x}O_4$	1.0 M KOH	50	400	8
N-doped graphene-CoO	1.0 M KOH	50	~440	9
$Zn_xCo_{3-x}O_4$ nanowire array	1.0 M KOH	50	390	10
Co-P films	1.0 M KOH	25	365	11
Co_3O_4/N -rmGO	1.0 M KOH	10	310	12
Co_3O_4@C-MWCNTs	1.0 M KOH	10	320	13
$Ni_xCo_{3-x}O_4$ nanowire	1.0 M KOH	10	370	14
NiCo LDH nanosheets	1.0 M KOH	10	367	15
$Ni_{0.5}Co_{0.5}O_x$	1.0 M KOH	10	360	16
CoCo LDH	1.0 M KOH	10	390	17
$Co_{0.5}Fe_{0.5}S$@N-MC	1.0 M KOH	10	410	18
Au@Co_3O_4/C	1.0 M KOH	10	380	19
Co_3O_4 /mMWCNT	1.0 M KOH	10	390	20
Mn_3O_4/$CoSe_2$	1.0 M KOH	10	450	21
$CoMoO_4$ nanorod	1.0 M KOH	10	343	22
$Ni_{30}Fe_7Co_{20}Ce_{43}O_x$	1.0 M KOH	10	410	23

Reference

1 M. Liu, X. Lu, C. Guo, Z. Wang, Y. Li, Y. Lin, Y. Zhou, S. Wang and J. Zhang, *ACS Appl. Mater. Interfaces*, 2017, **9**, 36146–36153.

2 T.-H. Lu, C.-J. Chen, Y.-R. Lu, C.-L. Dong and R.-S. Liu, *J. Phys. Chem. C*, 2016, **120**, 28093–28099.

3 G. McKendry, A. C. Thenuwara, J. Sun, H. Peng, J. P. Perdew, D. R. Strongin and M. J. Zdilla, *ACS Catal.*, 2016, **6**, 7393–7397.

4 X. Zhang, C. Si, X. Guo, R. Kong and F. Qu, *J. Mater. Chem. A*, 2017, **5**, 17211–17215.

5 N. Jiang, B. You, M. Sheng, Y. Sun, *Angew. Chem., Int. Ed.,* 2015, **54**, 6251–6254.

6 D. Liu, Q. Lu, Y. Luo, X. Sun, A. M. Asiri, *Nanoscale,* 2015, **7**, 15122–15126.

7 X. Liu, Z. Chang, L. Luo, T. Xu, X. Lei, J. Liu, X. Sun, *Chem. Mater.,* 2014, **6**, 1889–1895.

8 Z. Zhuang, W. Sheng, Y. Yan. *Adv. Mater,.* 2014, **26**, 3950–3955.

9 S. Mao, Z. Wen, T. Huang, Y. Hou and J. Chen, *Energy Environ. Sci.*, 2014, **7**, 609–616.

10 X. Liu, Z. Chang, L. Luo, T. Xu, X. Lei, J. Liu and X. Sun, *Chem. Mater.*, 2014, **26**, 1889–1895.

11 T. Liu, Y. Liang, Q. Liu, X. Sun, Y. H, A. M. Asiri, *Electrochem. Commun.,* 2015, 60, 92–96.

12 Y. Liang, Y. Li, H. Wang, J. Zhou, J. Wang, T. Regier and H. Dai, *Nat. Mater.*, 2011, **10,** 780–786.

13 X. Li, Y. Fang, X. Lin, M. Tian, X. An, Y. Fu, R. Li, J. Jin and J. Ma, *J. Mater. Chem. A*, 2015, **3**, 17392–17402.

14 Y. Li, P. Hasin and Y. Wu, *Adv. Mater.*, 2010, **22**, 1926–1929.

15 H. Liang, F. Meng, M. Caban-Acevedo, L. Li, A. Forticaux, L. Xiu, Z. Wang and S. Jin, *Nano Lett.*, 2015, **15**, 1421–1427.

16 L. Trotochaud, J. K. Ranney, K. N. Williams and S. W. Boettcher, *J. Am. Chem. Soc.*, 2012, **134**, 17253–17261.

17 F. Song and X. Hu, *Nat. Commun.*, 2014, **5**, 4477.

18 M. Shen, C. Ruan, Y. Chen, C. Jiang, K. Ai and L. Lu, *ACS Appl. Mater. Interfaces*, 2015, **7**, 1207–1218.

19 Z. Zhuang, W. Sheng and Y. Yan, *Adv. Mater.*, 2014, **26**, 3950–3955.

20 X. Lu, and C. Zhao, *J. Mater. Chem. A*, 2013, **1**, 12053–12059.

21 M. R. Gao, Y. F. Xu, J. Jiang, Y. R. Zheng and S. H. Yu, *J. Am. Chem. Soc.*, 2012, **134,** 2930–2933.

22 Q. Liu, A. M. Asiri and X. Sun, *Electrochem. Commun.,* 2014, **49**, 21–24.

23 S. Ratha, A. K. Samantara, K. K. Singha, A. S. Gangan, B. Chakraborty, B. K. Jena and C. S. Rout, *ACS Appl. Mater. Interfaces*, 2017, **9**, 9640–9653.